# A high resolution and quasi-zonal transect of dissolved Ba in the Mediterranean Sea

Stephanie Jacquet, Christophe Monnin, V Riou, Loïc Jullion, T Tanhua

# A high resolution and quasi zonal transect of dissolved Ba in the Mediterranean Sea

Jacquet S.H.M.[1], C. Monnin[2], V. Riou[1], L. Jullion[1] and T. Tanhua[3]

[1] Aix Marseille Université, CNRS/INSU, Université de Toulon, IRD, Mediterranean Institute of Oceanography (MIO), UM 110, 13288 Marseille, France

[2] Géosciences Environnement Toulouse, Université de Toulouse/CNRS/IRD/OMP, 14, Avenue Edouard Belin, 31400 Toulouse, France

[3] GEOMAR Helmholtz Centre for Ocean Research Kiel, Marine biogeochemistry, Kiel, Germany

Corresponding author: S. Jacquet, stephanie.jacquet@mio.osupytheas.fr

Key words: dissolved barium, barite saturation index, Mediterranean Sea

**Submitted to Marine Chemistry**

**Abstract**

The dissolved barium (D_Ba) data set for the Mediterranean Sea is here expanded with data from a large-scale transect sampled in April 2011 (M84/3 cruise) at high resolution. A total of 833 seawater samples have been analyzed for D_Ba. Over the basin the D_Ba content ranges from 38 to 85 nmol $kg^{-1}$ with local deep D_Ba maxima reaching up to 172 nmol $kg^{-1}$. Deep D_Ba maxima are associated with near bottom waters influenced by benthic processes and brine waters. The water column is largely undersaturated with respect to barite ($BaSO_4$, the main phase of particulate biogenic barium P_Ba), with water column barite saturation state ranging between 0.2 and 0.6 over the basin. This new D_Ba dataset shows that the general zonal distribution of D_Ba is impacted by the large-scale Mediterranean circulation, as evidenced by the Levantine Intermediate Water zonal and meridional progression as well as by the eastward flow of surface Atlantic Water. However biogeochemical processes are also at play, as suggested by an elevated D_Ba content of deep waters and by local lower D_Ba contents in intermediate waters. These features could be attributed to active cycling between the particulate and dissolved Ba phases. Since P_Ba barite has been recognized in previous studies as a proxy for particulate organic carbon remineralization at intermediate depths, the significance of local changes in the water column D_Ba patterns may be key to better constrain the Ba and carbon dynamics in the Mediterranean Sea.

## 1. Introduction

In the context of studies of the interactions between climate change and the oceanic biological carbon (C) pump, the barium (Ba) proxy is a key tracer to estimate the transfer of particulate matter and C from the water column to the sediments. Particulate biogenic barium (P_Ba) in suspended matter is mainly composed of barite ($BaSO_4$) crystals (Dehairs et al., 1980). Barite forms during particulate organic carbon (POC) degradation by marine prokaryotes at mesopelagic depths (100-1000 m; the depth range within which most of the POC transported from the mixed layer is degraded). In an ocean that is globally undersaturated with respect to barite (Monnin et al., 1999, Rushdi et al., 2000; Monnin and Cividini, 2006) POC sinking aggregates provide favourable microenvironments for barite precipitation. As a result, P_Ba barite is one of the few geochemical proxies for POC remineralization fluxes at mesopelagic depths (Dehairs et al., 1997, 2008; Cardinal et al., 2005; Jacquet et al., 2008, 2011, 2015).

It has been shown that dissolved Ba (D_Ba) behaves as a bio-intermediate element, i.e. showing low concentrations in surface waters without reaching total depletion and increasing concentrations with depth (Chan et al., 1977, Östlund et al., 1987; Jeandel et al., 1996; Jacquet et al., 2005). This distribution is mainly attributed to P_Ba cycling involving barite formation and dissolution. The Ba dynamics have been investigated in a previous study in the Southern Ocean by comparing temporal changes of dissolved and particulate barium contents and by calculating the degree of Ba conservation (Jacquet et al., 2007). It has been concluded that D_Ba displays a non-conservative behaviour at horizons of mesopelagic POC remineralization, pointing to a measureable removal of D_Ba

from the local seawater by barite formation (Jacquet et al., 2007). However, much remains unknown with regards to the significance of local changes in D_Ba patterns to further constrain Ba dynamics and POC transfer efficiency in the water column.

The Mediterranean Sea (MedSea) is a landlocked sea with limited, but crucial, exchange with the Atlantic Ocean, two deep overturning cells, one shallow circulation and a complex upper layer circulation with several permanent and quasi-permanent eddies. During the Holocene period (10.8 to 6.1 cal ka BP), the eastern Mediterranean suffered a major phase of climatic shift in thermohaline circulation causing abrupt changes in bottom water oxygenation and deposition of organic-rich anoxic sediment (sapropel). In the light of these past events, the biogeochemistry and dynamics of the circulation in the Western and Eastern Mediterranean (WMed, EMed), their connection and the possible implication for the regional climate system are thus key issues under debate (Tanhua et al., 2013b; Malanotte-Rizzoli).

The MedSea is also a basin of contrasting ecosystems, from strongly oligotrophic deep interiors to eutrophic northern Adriatic (Durrieu de Madron et al., 2011; Reygondeau et al., 2013). The coupling between surface biology and internal remineralization, timescales of their variability between sub-basins and discrepancies between mesopelagic trophic regime and respiration dynamics (Santinelli et al., 2010, 2014; Lopez-Sandoval et al., 2011; Luna et al., 2012) are for instance issues that need to be resolved for a better understanding of the bio-geochemical processes involved in the carbon dynamics of the Mediterranean basin. Open questions relates to the impact of the predicted changes in key physical (e.g. increased stratification, salinity) on this dynamics.

The present work provides a unique D_Ba dataset for the Mediterranean basin. The high sampling resolution offers unprecedented opportunity to discuss differences in the water column D_Ba distribution and the water column saturation with respect to barite between WMed and EMed, and to investigate the respective roles of physico-chemical and biogeochemical controls. This work is part of a broader investigation aiming at improving the use of Ba as a proxy to estimate local processes of POC remineralization in the Mediterranean Sea.

## 2. Experiment and methods

### 2.1 Study area

The whole water column was sampled for D_Ba along an east to west transect across the Mediterranean Sea from off the coast of Lebanon to the Strait of Gibraltar, enabling creation of a quasi-zonal section (M84/3 cruise, Istanbul to Vigo, 5-28 April 2011, R/V *Meteor*) (Figure 1) (Tanhua et al., 2013a). However, the Sicily Channel could not be sampled due to political instability in the region. Additionally, we present a short meridional section from the Adriatic Sea through the Strait of Otranto to the Ionian Sea (later referred to as the Ionian section). The period of the M84/3 cruise, April 2011, coincides with the end of the winter-spring bloom. The cruise was set up to follow the guide-lines of the GO-SHIP Program (Global Ocean Ship Based Hydrographic Investigation Program), which aims at creating a globally coordinated network of sustained hydrographic sections as part of the global ocean/climate observing system. The principal scientific objective for M84/3 was to understand and document large-scale Mediterranean water property distributions, their changes and the drivers of those changes. In particular, M84/3 focused on major shifts in the overturning

circulation of the Mediterranean basin which began at the end of the 1980s for the EMed (Roether et al., 1996) and in the mid-2000s for the WMed (Schroeder et al., 2008). Our specific objective was to document for the first time the D_Ba distribution in the Mediterranean basin at a large scale. D_Ba data are available in the CDIAC (Carbon Dioxide Information Analysis center) data repository, next to other physical and chemical parameters obtained during the M84/3 cruise (http://cdiac.ornl.gov/oceans/Coastal/Meteor_Med_Sea.html).

Detailed description of the Mediterranean circulation as well as water mass properties and distribution is given in Tanhua et al. (2013b) and Hainbucher et al. (2014). Briefly, the following main water masses can be distinguished (see potential temperature – salinity diagram in Fig.2; note that the mesopelagic layer is hereafter referred to as the intermediate layer): (1) the western part of the zonal section is dominated by the inflow of surface Atlantic Water (AW) associated with an intense meso-scale activity along the African coast, and the outflow of Mediterranean Overflow Water (MOW). AW is mainly detected by fresher waters; (2) from west to east, AW is gradually replaced by Ionian Surface Water (ISW) and Levantine Surface Water (LSW). LSW is formed by intensive heating and evaporation and has the highest salinity and temperature of the entire MedSea; (3) Levantine Intermediate Water (LIW) is present at intermediate layers over the whole basin and represents the intermediate water mass connection between sub-basins. LIW is characterized by high density and a salinity maximum. During the M84/3 cruise, the core of LIW was detected around 200 m depth in the EMed and around 500 m depth in the WMed. Cretan Intermediate Water (CIW) is also found at intermediate depths in the EMed; (4) in the deep waters we find Eastern Mediterranean Deep Water (EMDW) and Western

Mediterranean Deep Water (WMDW), in each sub-basin. EMDW is a mixture of Adriatic Deep Water (AdDW), Cretan Deep Water (CDW) and shallower water masses. WMDW is mainly formed in the Gulf of Lion by open-ocean convection (Schott et al., 1996) with intermittent contribution from shelf water cascading (Durrieu de Madron et al., 2013).

**2.2 Sampling and analyses**

Seawater was sampled with a CTD rosette equipped with 24 12-liter water bottles. Then, fifteen mL of unfiltered seawater were collected in pre-cleaned polypropylene bottles (Nalgene; rinsed three times with the same seawater sample), acidified with 15 µL of HCl (Optima grade) and kept at room temperature for later analysis. No filtration of the seawater was done based on the well-documented knowledge that D_Ba represents, in general, a very large fraction (>99%) of total Ba. There were 47 vertical D_Ba profiles with a total of 833 D_Ba samples.

D_Ba was measured using an isotope dilution (ID) method (Klinkhammer and Chan, 1990 and Freydier et al., 1995) by high resolution sector field - inductively coupled plasma- mass spectrometry (SF-ICP-MS). This method was adapted to a Thermo Finnigan Element XR instrument. The D_Ba measurements presented here are the sum of dissolved Ba (D_Ba) and a very small fraction (generally <1% of total Ba) that is generated from the particulate Ba pool as a result of the acidification. For the sake of simplicity, we use the term of D_Ba. Samples (0.5 mL) were spiked with 300 µL of a $^{135}$Ba-enriched solution (93% $^{135}$Ba; 95 nmol kg$^{-1}$), and 300 µL of a Nd solution (natural isotopic composition; 70 nmol kg$^{-1}$) was added as an internal standard to correct for mass bias. Finally,

samples were diluted with 15 mL of acidified (2% $HNO_3$, Optima grade) Milli-Q grade water. The amount of sample, spikes and dilution water were assessed by weighing. Reproducibility of this method is 1.5% (RSD) as tested on repeated preparations of reference solutions: SLRS-5 (NRC-CNRC river water reference material for trace metals; 101.9 ± 3.6 nmol $kg^{-1}$) and a house-made reference of Mediterranean Sea water (deep water from the MOOSE DYFAMED site; 54.1 nmol $kg^{-1}$). The limit of detection, calculated as three times the standard deviation of the procedural blank, is 0.09 nmol $kg^{-1}$.

Using the D_Ba concentration, temperature, pressure and salinity data from the M84/3 cruise, we calculated the barite saturation index (SI) following the procedures described by Monnin et al. (1999) and Monnin and Cividini (2006). SI is defined as the Q/K ratio, where Q is the ionic product of aqueous barium sulphate, and K is the solubility product of barite. A saturation index value between 0.9 and 1.1 is taken to represent equilibrium (Monnin et al., 1999). Waters are considered to be undersaturated for SI <0.9.

## 3. RESULTS

Figure 3 shows the full-depth D_Ba distribution for the Ionian and zonal sections, with the top 500 m expanded. The same scheme is reported for the barite saturation index (SI) in Figure 4. Figure 5 shows characteristic vertical D_Ba profiles for the major sub-basins, as well as D_Ba profiles for stations not included in the Ionian and zonal sections. Two broad features characterize the D_Ba in the Mediterranean Sea: 1) a vertical gradient increasing from 38 nmol $kg^{-1}$ near the surface to 85 nmol $kg^{-1}$ at the bottom, with local deep D_Ba maxima reaching up to 172 nmol $kg^{-1}$, and 2) a pronounced water column undersaturation

with respect to barite ($0.2 \leq SI \leq 0.6$) with a relative maximum in the intermediate waters at around 500 meters depth.

West of Gibraltar, in the Gulf of Cadiz, D_Ba concentrations range from 38 to 55 nmol $kg^{-1}$ in highly undersaturated waters (SI from 0.2 to 0.4) with only small vertical gradients (see representative D_Ba profile at station #340 in Figure 5a). The low D_Ba and SI characteristic of AW can be followed throughout the surface waters of the Mediterranean Sea. For the upper 1000 m in the WMed, the D_Ba distribution is marked by increasing D_Ba concentration <70 nmol $kg^{-1}$ from west to east. In the EMed, the intermediate layer (200 to 700 m depth) is marked by slightly lower D_Ba concentration (50 to 70 nmol $kg^{-1}$) between 17 and 26°E.

The deep (>1000 m) layers of the Mediterranean Sea are characterized by D_Ba concentrations above 70 nmol $kg^{-1}$ with localized patches peaking up to 100 nmol $kg^{-1}$. Those are observed at 9.4°E in the WMed (station #321) and at 27.5°E in the EMed (station # 290) (see D_Ba profiles in Figure 5f). Very high D_Ba concentrations (139 and 172 nM, respectively) are furthermore found near the bottom at 33°E (station #291) and 21.5°E (station #301) (see D_Ba profiles in Figure 5g). Note that very high D_Ba contents (up to 160 nmol $kg^{-1}$) are also found near the bottom at station #288 located at 26.2°E north-east of Crete (not shown in the zonal section; see D_Ba profile in Figure 5g).

The same general features as reported for the zonal section are observed across the Ionian section, where the D_Ba distribution is also marked by an increase in the water column D_Ba content (from 48 to 95 nmol $kg^{-1}$) in undersaturated waters (SI from 0.3 to 0.5). A SI maximum again extends in intermediate waters and lower D_Ba concentrations (<70 nmol $kg^{-1}$) occur

between 500 and 800 m along the Ionian section. The northern part of the Ionian section, north of the Otranto Strait (Adriatic Pit), is marked by relatively homogeneous D_Ba concentrations (<65 nmol $kg^{-1}$) below 300 m (see D_Ba profile at station #313 in Figure 5c). Also, a particular D_Ba increase (up to 95 nmol $L^{-1}$) is observed around a depth of 2000 m (station #307; see D_Ba profile in Figure 5c). Note that a similar increase in D_Ba concentrations around the same depth is detected at station #314 located in the area of station #307 (not shown in Fig.3; see D_Ba profile in Figure 5c). D_Ba increase around a depth of 2000 m is also observed in the EMed at stations #303 (southern Ionan Sea) and at stations #300 (24.3°E) and #298 (22.5°E) (not shown in Fig.3; see D_Ba profiles in Figure 5d).

## 4. DISCUSSION

D_Ba concentrations reported in the present work (from 38 to 100 nmol $kg^{-1}$) are of the same order of magnitude as D_Ba values reported during previous Mediterranean cruises in the EMed (GEODYME data, Jeandel et al., pers. comm.) and in the WMed (Bernat et al., 1972; Dehairs et al., 1987; van Beek et al., 2009). Previous MedSea data are however relatively scarce, with in general limited vertical sampling resolution, preventing direct comparisons with the present data set. D_Ba concentrations for the MedSea are also of the same order of magnitude as values reported for the Atlantic sector (Chan et al., 1977), the Indian and Southern Oceans (Jeandel et al., 1996; Jacquet et al., 2004, 2007, Hoppema et al., 2010) and for the North Pacific (Dehairs et al., 2008). Compared to the previous sectors, D_Ba concentrations in the MedSea present however smaller vertical D_Ba gradients which mainly range from 38 to 85 nmol $kg^{-1}$ between the surface

and the bottom. Our results indicate that the MedSea is undersaturated with respect to barite everywhere, in contrast to the above-mentioned oceans where saturation can be reached at certain locations (Monnin et al., 1999; Dehairs et al., 2008; Jacquet et al., 2008). SI exhibits a maximum value at depths around 500 m. Below these depths, the variations in D_Ba concentration and temperature are small. The only factor affecting the SI value is pressure. The increase with pressure of the barite solubility product (K) is much larger than the increase of the aqueous barium sulphate ionic product (Q) which is proportional to the square of the activity coefficient of aqueous barium sulphate (Monnin et al., 1999; Monnin and Cividini, 2006). This results in a decrease of the barite SI with depth at depth ranges where D_Ba and temperature are almost constant (i.e. the variations are too low to affect SI).

For the upper 1000 m, the general zonal D_Ba pattern appears influenced by the water circulation in the Mediterranean basin. In the western part of the transect, the low D_Ba contents and SI values coincide with the low-salinity surface AW flowing through the Strait of Gibraltar. The transition between AW and underlying LIW (referred to as MOW in the Gibraltar Strait) is marked by a steep vertical D_Ba gradient (D_Ba concentrations from <55 to >70 nmol $kg^{-1}$). In the northern part of the Ionian section, the relatively homogeneous D_Ba concentrations (at values <65 nmol $kg^{-1}$) below 300 m result from the transition above the Otranto Strait from northward progressing LIW to less salty Adriatic waters potentially influenced by riverine input. Between 17 and 26°E in the EMed, low D_Ba values (D_Ba contents from 50 to 70 nmol $kg^{-1}$) coincide in the upper 400 m with the sinking and westward progression of high density LIW (salinity maximum between 200 and 500 m). The sinking of isolines from east to

west in this zone is a feature also observed for other water mass properties (salinity, temperature, potential density and nutrients) (Tanhua et al., 2013b). It is furthermore possible that the extent of lower D_Ba concentrations down to 700 m in this area reflects D_Ba subtraction due to P_Ba barite formation. The same is true for the lower D_Ba concentrations reported along the Ionian section between 500 and 800 m.

Concerning the deeper (>1000 m) water column, the high values of D_Ba reported at 9.4°E and 27.5°E (up to 100 nmol $kg^{-1}$) coincide with the top of seamounts. This Ba enrichment may be due to local dissolution of Ba-rich particles (barite) in the under-saturated water and would reflect epibenthic fluxes of Ba-rich particles that have been exported from the intermediate layers to the sea floor. This may also occur at station #291 (33°E) where the high D_Ba value of 139 nmol $kg^{-1}$ is found near the seafloor. The same is true for station #288 (north-east of Crete) where D_Ba concentrations near the seafloor reach 160 nmol $kg^{-1}$. Another source of very high D_Ba concentrations in the MedSea could originate from the Black Sea where Moore and Falkner (1999) reported water column D_Ba concentrations ranging from 130 to 500 nmol $kg^{-1}$. No particularly high water column D_Ba concentration is however reported at station #287 in the southern Eagean Sea, nor further south at station #289 located in the area of station #288 north-east of Crete (Fig.5e). A particular situation is also encountered at 21.5°E (station #301) where the highest D_Ba concentration (172 nmol $kg^{-1}$) of the whole dataset is found close to the "Atalante" brine lake, a water body with very high salinity (up to 160) and anoxic conditions. It has been well established that brines are highly concentrated in various elements (e.g. trace metals). Extremely high D_Ba contents (up 670 nmol $kg^{-1}$) resulting from sulphate salt

dissolution have for instance been reported in the Orca basin (Gulf of Mexico) (Schijf, 2007). The high D_Ba contents reported at 21.5°E (station #301) in the EMed do not therefore reflect a higher export of Ba-rich particles to the seafloor, benthic processes, nor a possible influence of Black Sea waters, but rather an influence of the nearby brine lake.

The observed D_Ba variation with depth (surface depletion and depth enrichment) is often referred to as a nutrient-like distribution. The precise mechanism shaping this D_Ba distribution is still debated mainly because the control on barite formation inside POC micro-environments in undersaturated ocean waters is not fully resolved (Griffith and Paytan, 2012). The nutrient distribution during M84/3 (late winter-spring) is characterized by very low concentrations, in particular in the EMed (Tanhua et al., 2013b). The same trend was reported in previous studies emphasizing the increasing oligotrophic trend from west to east along the basin (Moutin and Raimbault, 2002; Pujo-Pay et al., 2011). The D_Ba distribution is more uniform between WMed and EMed during M84/3 than reported for nutrients (Tanhua et al., 2013b). Also, the D_Ba distribution is not fully depleted in surface waters and presents specific local depletions at intermediate depths. Jeandel et al. (1996) and Jacquet et al. (2007) reported a decoupling between D_Ba and silicate and alkalinity distributions in the water column due to the fact that D_Ba is not controlled by the same biogeochemical processes as those controlling the synthesis of opal and carbonate, and their dissolution. Throughout the whole basin, while barite is undersaturated, calcite and aragonite are largely supersaturated (Alvarez et al., 2014). This would explain decoupling between D_Ba and total alkalinity in the deep waters (not shown; see Alvarez et al., 2014), as reflected by increasing D_Ba concentrations

despite constant total alkalinity in the water column below 1000 m, especially in the EMed. The D_Ba enrichment in deep waters reflects dissolution of Ba-rich particles produced at intermediate depths and exported to the sea floor. This D_Ba increase may be enhanced by the residence time and ventilation of deep waters. Studies of transient tracers (CFC-12, $SF_6$ and tritium) over the last two decades revealed a period of low ventilation in the deep eastern (Levantine) basin, while the WMed was marked by massive input of recently ventilated water (Ströven and Tanhua, 2013; Schneider et al., 2014; Schröder et al., 2008, 2010). These differences in the ventilation of deep water masses could explain the fact that the extent of high D_Ba values is larger in the EMed than in the WMed. Nevertheless, the fact that over the basin the D_Ba concentration increases with depth indicates dissolution of Ba-rich particles produced at intermediate depths during POC remineralization processes and transferred through the deep water. Our results indicate that this transfer of Ba-rich particles is more important at 9°E in the WMed and east of 25°E in the EMed (i.e. D_Ba contents >80 nmol $kg^{-1}$). The particulate and dissolved organic carbon (POC, DOC) dynamics in the MedSea are relatively complex (Lefèvre et al., 1996; Santinelli et al., 2010; Lopez-Sandoval et al., 2011; Luna et al., 2012). It is therefore difficult to discuss in detail the link between the deep water column transfer of Ba-enriched particles and sinking POC.

## 5. CONCLUSION

The present paper presents an extended data set on the D_Ba distribution along a high resolution and quasi-zonal transect in the MedSea in late winter-spring 2011. Our results reveal that the D_Ba distribution appears driven by

hydrodynamics, while enhanced D_Ba contents in deep waters could reflect the effect of a higher P_Ba barite flux in undersaturated water. Also, the occurrence of lower D_Ba contents at intermediate depths could reflect horizons of intense particulate and dissolved Ba dynamics. In order to further constrain the link between these specific features of the D_Ba distribution and the organic carbon dynamics in the MedSea, the sensitivity of the Ba signal to the phytoplankton growth season and to dense-water formation events should be addressed.

**Acknowledgements**

For their support to this research, we thank the captain and crew of R/V *Meteor*. R. Brünjes (GEOMAR) took the barium samples during the M84/3 cruise. S. Chifflet (MIO) helped for samples processing. This research was supported by French LEFE CYBER grant (BADIMED project; 2014-2015). The HR-ICP-MS (ELEMENT XR, Thermo) was supported in 2012 by European Regional Development Fund (ERDF). The M84/3 cruise was supported by a grant from the Deutsche Forschungsgemeinschaft (DFG)- Senatskommission für Ozeanographie, and from a grant from DFG [TA 317/3-1]. Authors thank the Labex OT- Med (ANR-11-LABEX-0061) funded by the « Investissements d'Avenir », French Government project of the French National Research Agency (ANR) through the A*Midex project (ANR-11-IDEX-0001-02), for enhancing networking of the BADIMED project. LJ acknowledges the support of the European Union via a Marie Curie fellowship (FP7-PEOPLE-2012-IEF no 328416).

**Figure captions**

Figure 1: Map of the Mediterranean Sea with the stations (blue dots) of the M84/3 cruise where samples were taken for the analysis of dissolved barium, along with the bathymetry of the basins. WMED: Western Mediterranean Sea, EMED: Eastern Mediterranean Sea. Figure constructed using Ocean Data View (Schlitzer, 2003).

Figure 2: Potential temperature – salinity diagram with isopycnals (kg $m^{-3}$) of the whole data set (a) and focus on deep waters (b). Colors represent the concentration of D_Ba in nmol $kg^{-1}$. WMed, EMed: Western and Eastern Mediterranean Sea. AW= Atlantic Water, MOW= Mediterranean Overflow Water, ISW= Ionian Surface Water, LSW= Levantine Surface Water, LIW= Levantine Intermediate Water, CIW= Cretan Intermediate Water, WMDW= Western Mediterranean Deep Water, AdDW= Adriatic Deep Water, CDW= Cretan Deep Water.

Figure 3: Sections of D_Ba distribution (nmol $kg^{-1}$) in the Mediterranean Sea from the Meteor cruise M84/3 (April 2011). The top-right panel is a meridional section from the Adriactic Sea to the Ionian sea (light grey line on the map) and the lower panel is the zonal section from the coast of Lebanon in the EMed to the Strait of Gibraltar in the WMed (dark grey line on the map). The depth scale and the color scale are identical for all panels. The top 500 m in each section and associated color scale are slightly expanded.

Figure 4: Similar to Fig.3, but for barite saturation index (SI).

Figure 5: Characteristic vertical D_Ba profiles for the major sub-basins and D_Ba profiles for stations not included in the Ionian and zonal sections.

**References**


Álvarez, M., Sanleón-Bartolomé, H., Tanhua, T., Mintrop, L., Luchetta, A., Cantoni, C., Schroeder, K., Civitarese, G., 2014. The CO2 system in the Mediterranean Sea: a basin wide perspective. Ocean Sci. 10, 69–92. doi:10.5194/os-10-69-2014

Bernat, M., Church, T., Allegre, C.J., 1972. Barium and strontium concentrations in Pacific and Mediterranean sea water profiles by direct isotope dilution mass spectrometry. Earth and Planetary Science Letters 16, 75–80. doi:10.1016/0012-821X(72)90238-5

Cardinal, D., Savoye, N., Trull, T.W., André, L., Kopczynska, E.E., Dehairs, F., 2005. Variations of carbon remineralisation in the Southern Ocean illustrated by the Baxs proxy. Deep Sea Research Part I: Oceanographic Research Papers 52, 355–370. doi:10.1016/j.dsr.2004.10.002

Chan, L.H., Drummond, D., Edmond, J.M., Grant, B., 1977. On the barium data from the Atlantic GEOSECS expedition. Deep Sea Research 24, 613–649. doi:10.1016/0146-6291(77)90505-7

Dehairs, F., Chesselet, R., Jedwab, J., 1980. Discrete suspended particles of barite and the barium cycle in the open ocean. Earth and Planetary Science Letters 49, 528–550. doi:10.1016/0012-821X(80)90094-1

Dehairs, F., Jacquet, S., Savoye, N., Van Mooy, B.A.S., Buesseler, K.O., Bishop, J.K.B., Lamborg, C.H., Elskens, M., Baeyens, W., Boyd, P.W., Casciotti,

K.L., Monnin, C., 2008. Barium in twilight zone suspended matter as a potential proxy for particulate organic carbon remineralization: Results for the North Pacific. Deep Sea Research Part II: Topical Studies in Oceanography, Understanding the Ocean's Biological Pump:results from VERTIGO 55, 1673–1683. doi:10.1016/j.dsr2.2008.04.020

Dehairs, F., Lambert, C.E., Chesselet, R., Risler, N., 1987. The biological production of marine suspended barite and the barium cycle in the Western Mediterranean Sea. Biogeochemistry 4, 119–140. doi:10.1007/BF02180151

Dehairs, F., Shopova, D., Ober, S., Veth, C., Goeyens, L., 1997. Particulate barium stocks and oxygen consumption in the Southern Ocean mesopelagic water column during spring and early summer: relationship with export production. Deep Sea Research Part II: Topical Studies in Oceanography 44, 497–516. doi:10.1016/S0967-0645(96)00072-0

Durrieu de Madron, X., Guieu, C., Sempéré, R., Conan, P., Cossa, D., D'Ortenzio, F., Estournel, C., Gazeau, F., Rabouille, C., Stemmann, L., Bonnet, S., Diaz, F., Koubbi, P., Radakovitch, O., Babin, M., Baklouti, M., Bancon-Montigny, C., Belviso, S., Bensoussan, N., Bonsang, B., Bouloubassi, I., Brunet, C., Cadiou, J.-F., Carlotti, F., Chami, M., Charmasson, S., Charrière, B., Dachs, J., Doxaran, D., Dutay, J.-C., Elbaz-Poulichet, F., Eléaume, M., Eyrolles, F., Fernandez, C., Fowler, S., Francour, P., Gaertner, J.C., Galzin, R., Gasparini, S., Ghiglione, J.-F., Gonzalez, J.-L., Goyet, C., Guidi, L., Guizien, K., Heimbürger, L.-E., Jacquet, S.H.M., Jeffrey, W.H., Joux, F., Le Hir, P., Leblanc, K., Lefèvre, D., Lejeusne, C., Lemé, R., Loÿe-Pilot, M.-D., Mallet, M., Méjanelle, L., Mélin, F., Mellon, C., Mérigot, B., Merle, P.-L., Migon, C., Miller, W.L., Mortier, L., Mostajir, B., Mousseau, L., Moutin, T., Para,

J., Pérez, T., Petrenko, A., Poggiale, J.-C., Prieur, L., Pujo-Pay, M., Pulido-Villena, Raimbault, P., Rees, A.P., Ridame, C., Rontani, J.-F., Ruiz Pino, D., Sicre, M.A., Taillandier, V., Tamburini, C., Tanaka, T., Taupier-Letage, I., Tedetti, M., Testor, P., Thébault, H., Thouvenin, B., Touratier, F., Tronczynski, J., Ulses, C., Van Wambeke, F., Vantrepotte, V., Vaz, S., Verney, R., 2011. Marine ecosystems' responses to climatic and anthropogenic forcings in the Mediterranean. Progress in Oceanography 91, 97–166. doi:10.1016/j.pocean.2011.02.003

Freydier, R., Dupre, B., Polve, M., 1995. Analyses by Inductively-Coupled Plasma-Mass Spectrometry of Ba Concentrations in Water and Rock Samples - Comparison Between Isotope-Dilution and External Calibration with or Without Internal Standard. Eur. Mass Spectrom. 1, 283–291. doi:10.1255/ejms.140

Griffith, E.M., Paytan, A., 2012. Barite in the ocean – occurrence, geochemistry and palaeoceanographic applications. Sedimentology 59, 1817–1835. doi:10.1111/j.1365-3091.2012.01327

Durrieu de Madron, X., Houpert, L., Puig, P., Sanchez-Vidal, A., Testor, P., Bosse, A., Estournel, C., Somot, S., Bourrin, F., Bouin, M.N., Beauverger, M., Beguery, L., Calafat, A., Canals, M., Cassou, C., Coppola, L., Dausse, D., D'Ortenzio, F., Font, J., Heussner, S., Kunesch, S., Lefevre, D., Le Goff, H., Martín, J., Mortier, L., Palanques, A., Raimbault, P., 2013. Interaction of dense shelf water cascading and open-sea convection in the northwestern Mediterranean during winter 2012. Geophys. Res. Lett. 40, 1379–1385. doi:10.1002/grl.50331

Hainbucher, D., Rubino, A., Cardin, V., Tanhua, T., Schroeder, K., Bensi, M., 2014. Hydrographic situation during cruise M84/3 and P414 (spring 2011) in the Mediterranean Sea. Ocean Sci. 10, 669–682. doi:10.5194/os-10-669-2014

Hoppema, M., Dehairs, F., Navez, J., Monnin, C., Jeandel, C., Fahrbach, E., de Baar, H.J.W., 2010. Distribution of barium in the Weddell Gyre: Impact of circulation and biogeochemical processes. Marine Chemistry 122, 118–129. doi:10.1016/j.marchem.2010.07.005

Jacquet, S.H.M., Dehairs, F., Cardinal, D., Navez, J., Delille, B., 2005. Barium distribution across the Southern Ocean frontal system in the Crozet–Kerguelen Basin. Marine Chemistry 95, 149–162. doi:10.1016/j.marchem.2004.09.002

Jacquet, S.H.M., Dehairs, F., Dumont, I., Becquevort, S., Cavagna, A.-J., Cardinal, D., 2011. Twilight zone organic carbon remineralization in the Polar Front Zone and Subantarctic Zone south of Tasmania. Deep Sea Research Part II: Topical Studies in Oceanography, Biogeochemistry of the Australian Sector of the Southern Ocean 58, 2222–2234. doi:10.1016/j.dsr2.2011.05.029

Jacquet, S.H.M., Dehairs, F., Elskens, M., Savoye, N., Cardinal, D., 2007. Barium cycling along WOCE SR3 line in the Southern Ocean. Marine Chemistry, Special issue: Dedicated to the memory of Professor Roland Wollast 106, 33–45. doi:10.1016/j.marchem.2006.06.007

Jacquet, S.H.M., Dehairs, F., Lefèvre, D., Cavagna, A.J., Planchon, F., Christaki, U., Monin, L., André, L., Closset, I., Cardinal, D., 2015. Early spring mesopelagic carbon remineralization and transfer efficiency in the naturally

iron-fertilized Kerguelen area. Biogeosciences 12, 1713–1731. doi:10.5194/bg-12-1713-2015

Jacquet, S.H.M., Dehairs, F., Rintoul, S., 2004. A high resolution transect of dissolved barium in the Southern Ocean. Geophys. Res. Lett. 31, L14301. doi:10.1029/2004GL020016

Jacquet, S.H.M., Dehairs, F., Savoye, N., Obernosterer, I., Christaki, U., Monnin, C., Cardinal, D., 2008. Mesopelagic organic carbon remineralization in the Kerguelen Plateau region tracked by biogenic particulate Ba. Deep Sea Research Part II: Topical Studies in Oceanography, KEOPS: Kerguelen Ocean and Plateau compared Study 55, 868–879. doi:10.1016/j.dsr2.2007.12.038

Jeandel, C., Dupré, B., Lebaron, G., Monnin, C., Minster, J.-F., 1996. Longitudinal distributions of dissolved barium, silica and alkalinity in the western and southern Indian Ocean. Deep Sea Research Part I: Oceanographic Research Papers 43, 1–31. doi:10.1016/0967-0637(95)00098-4

Klinkhammer, G.P., Chan, L.H., 1990. Determination of barium in marine waters by isotope dilution inductively coupled plasma mass spectrometry. Analytica Chimica Acta 232, 323–329. doi:10.1016/S0003-2670(00)81249-0

Lefévre, D., Denis, M., Lambert, C.E., Miquel, J.-C., 1996. Is DOC the main source of organic matter remineralization in the ocean water column? Journal of Marine Systems, The Coastal Ocean in a Global Change Perspective 7, 281–291. doi:10.1016/0924-7963(95)00003-8

López-Sandoval, D.C., Fernández, A., Marañón, E., 2011. Dissolved and particulate primary production along a longitudinal gradient in the Mediterranean Sea. Biogeosciences 8, 815–825. doi:10.5194/bg-8-815-2011

Luna, G.M., Bianchelli, S., Decembrini, F., De Domenico, E., Danovaro, R., Dell'Anno, A., 2012. The dark portion of the Mediterranean Sea is a bioreactor of organic matter cycling. Global Biogeochem. Cycles 26, GB2017. doi:10.1029/2011GB004168

Malanotte-Rizzoli, P., Artale, V., Borzelli-Eusebi, G.L., Brenner, S., Crise, A., Gacic, M., Kress, N., Marullo, S., Ribera d'Alcalà, M., Sofianos, S., Tanhua, T., Theocharis, A., Alvarez, M., Ashkenazy, Y., Bergamasco, A., Cardin, V., Carniel, S., Civitarese, G., D'Ortenzio, F., Font, J., Garcia-Ladona, E., Garcia-Lafuente, J.M., Gogou, A., Gregoire, M., Hainbucher, D., Kontoyannis, H., Kovacevic, V., Kraskapoulou, E., Kroskos, G., Incarbona, A., Mazzocchi, M.G., Orlic, M., Ozsoy, E., Pascual, A., Poulain, P.-M., Roether, W., Rubino, A., Schroeder, K., Siokou-Frangou, J., Souvermezoglou, E., Sprovieri, M., Tintoré, J., Triantafyllou, G., 2014. Physical forcing and physical/biochemical variability of the Mediterranean Sea: a review of unresolved issues and directions for future research. Ocean Science 10, 281–322. doi:10.5194/os-10-281-2014

Monnin, C., Cividini, D., 2006. The saturation state of the world's ocean with respect to (Ba,Sr)SO4 solid solutions. Geochimica et Cosmochimica Acta 70, 3290–3298. doi:10.1016/j.gca.2006.04.002

Monnin, C., Jeandel, C., Cattaldo, T., Dehairs, F., 1999. The marine barite saturation state of the world's oceans. Marine Chemistry 65, 253–261. doi:10.1016/S0304-4203(99)00016-X

Moore, W.S., Falkner, K.K., 1999. Cycling of radium and barium in the Black Sea. Journal of Environmental Radioactivity 43, 247–254. doi:10.1016/S0265-931X(98)00095-2

Ostlund, H.G., et al, 1987. GEOSECS Atlantic, Pacific, and Indiean Ocean Expeditions Vol 7 [WWW Document]. EPIC3Washington, D.C., NSF. URL http://epic.awi.de/34890/ (accessed 4.13.15).

Reygondeau, G, Irisson J-O, Guieu C, Gasparini S, Ayata, S-D, P. Koubbi, 2013. Toward a dynamic biogeochemical division of the Mediterranean Sea in a context of global climate change. EGU General Assembly 2013, Vienna, Austria, 07–12 April 2013. Available at: http://meetingorganizer.copernicus.org/EGU2013/EGU2013-10011.pdf.

Roether, W., Manca, B.B., Klein, B., Bregant, D., Georgopoulos, D., Beitzel, V., Kovačević, V., Luchetta, A., 1996. Recent Changes in Eastern Mediterranean Deep Waters. Science 271, 333–335. doi:10.1126/science.271.5247.333

Rushdi, A.I., McManus, J., Collier, R.W., 2000. Marine barite and celestite saturation in seawater. Marine Chemistry 69, 19–31. doi:10.1016/S0304-4203(99)00089-4

Santinelli, C., Nannicini, L., Seritti, A., 2010. DOC dynamics in the meso and bathypelagic layers of the Mediterranean Sea. Deep Sea Research Part II: Topical Studies in Oceanography, Ecological and Biogeochemical Interactions in the Dark Ocean 57, 1446–1459. doi:10.1016/j.dsr2.2010.02.014

Schijf, J., 2007. Alkali elements (Na, K, Rb) and alkaline earth elements (Mg, Ca, Sr, Ba) in the anoxic brine of Orca Basin, northern Gulf of Mexico. Chemical Geology 243, 255–274. doi:10.1016/j.chemgeo.2007.06.011

Schlitzer, R., 2003. Ocean Data View, http://www.awi-bremerhaven.de/GEO/ODV

Schneider, A., Tanhua, T., Roether, W., Steinfeldt, R., 2014. Changes in ventilation of the Mediterranean Sea during the past 25 year. Ocean Sci. 10, 1–16. doi:10.5194/os-10-1-2014

Schott, F., Visbeck, M., Send, U., Fischer, J., Stramma, L., Desaubies, Y., 1996. Observations of Deep Convection in the Gulf of Lions, Northern Mediterranean, during the Winter of 1991/92. Journal of Physical Oceanography 26, 505–524. doi:10.1175/1520-0485(1996)026<0505:OODCIT>2.0.CO;2

Schroeder, K., Josey, S.A., Herrmann, M., Grignon, L., Gasparini, G.P., Bryden, H.L., 2010. Abrupt warming and salting of the Western Mediterranean Deep Water after 2005: Atmospheric forcings and lateral advection. J. Geophys. Res. 115, C08029. doi:10.1029/2009JC005749

Schroeder, K., Ribotti, A., Borghini, M., Sorgente, R., Perilli, A., Gasparini, G.P., 2008. An extensive western Mediterranean deep water renewal between 2004 and 2006. Geophys. Res. Lett. 35, L18605. doi:10.1029/2008GL035146

Shopova, D., Dehairs, F., Baeyens, W., 1995. A simple model of biogeochemical element distribution in the oceanic water column. Journal of Marine Systems 6, 331–344. doi:10.1016/0924-7963(94)00032-7

Stöven, T., Tanhua, T., 2014. Ventilation of the Mediterranean Sea constrained by multiple transient tracer measurements. Ocean Sci. 10, 439–457. doi:10.5194/os-10-439-2014

Tanhua, T., Hainbucher, D., Cardin, V., Álvarez, M., Civitarese, G., McNichol, A.P., Key, R.M., 2013a. Repeat hydrography in the Mediterranean Sea, data

from the <i>Meteor</i> cruise 84/3 in 2011. Earth System Science Data 5, 289–294. doi:10.5194/essd-5-289-2013

Tanhua, T., Hainbucher, D., Schroeder, K., Cardin, V., Álvarez, M., Civitarese, G., 2013b. The Mediterranean Sea system: a review and an introduction to the special issue. Ocean Sci. 9, 789–803. doi:10.5194/os-9-789-2013

Van Beek, P., Sternberg, E., Reyss, J.-L., Souhaut, M., Robin, E., Jeandel, C., 2009. 228Ra/226Ra and 226Ra/Ba ratios in the Western Mediterranean Sea: Barite formation and transport in the water column. Geochimica et Cosmochimica Acta 73, 4720–4737. doi:10.1016/j.gca.2009.05.063

**Figure2**

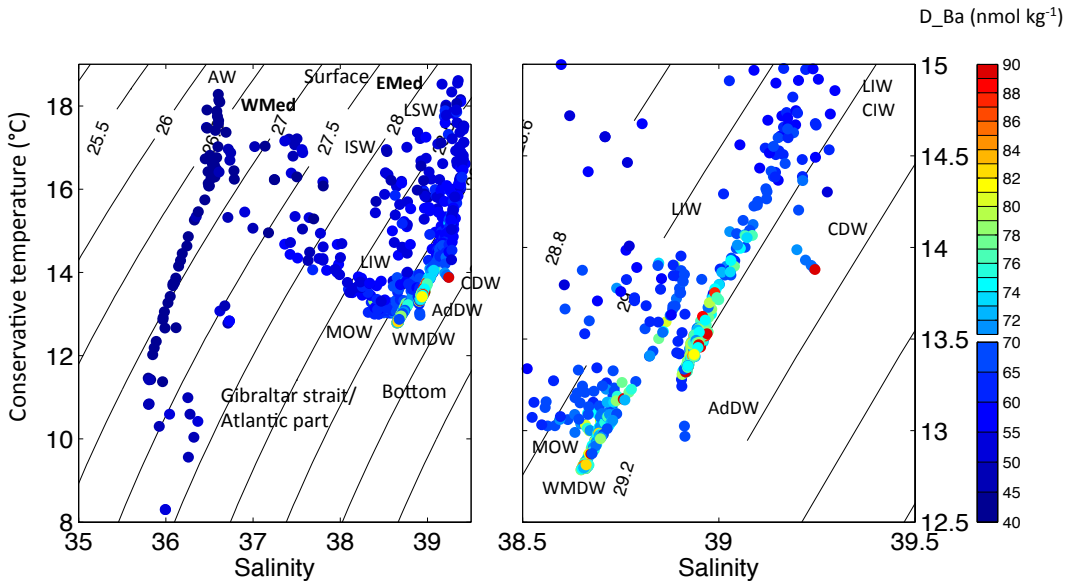
D_Ba (nmol kg-1)
Conservative temperature (°C)
Salinity
Salinity
AW
WMed
Surface
EMed
LSW
ISW
LIW
CDW
AdDW
MOW
WMDW
Gibraltar strait/
Atlantic part
Bottom
CIW
25.5
26
26.5
27
27.5
28
28.8
29
29.2

Figure3

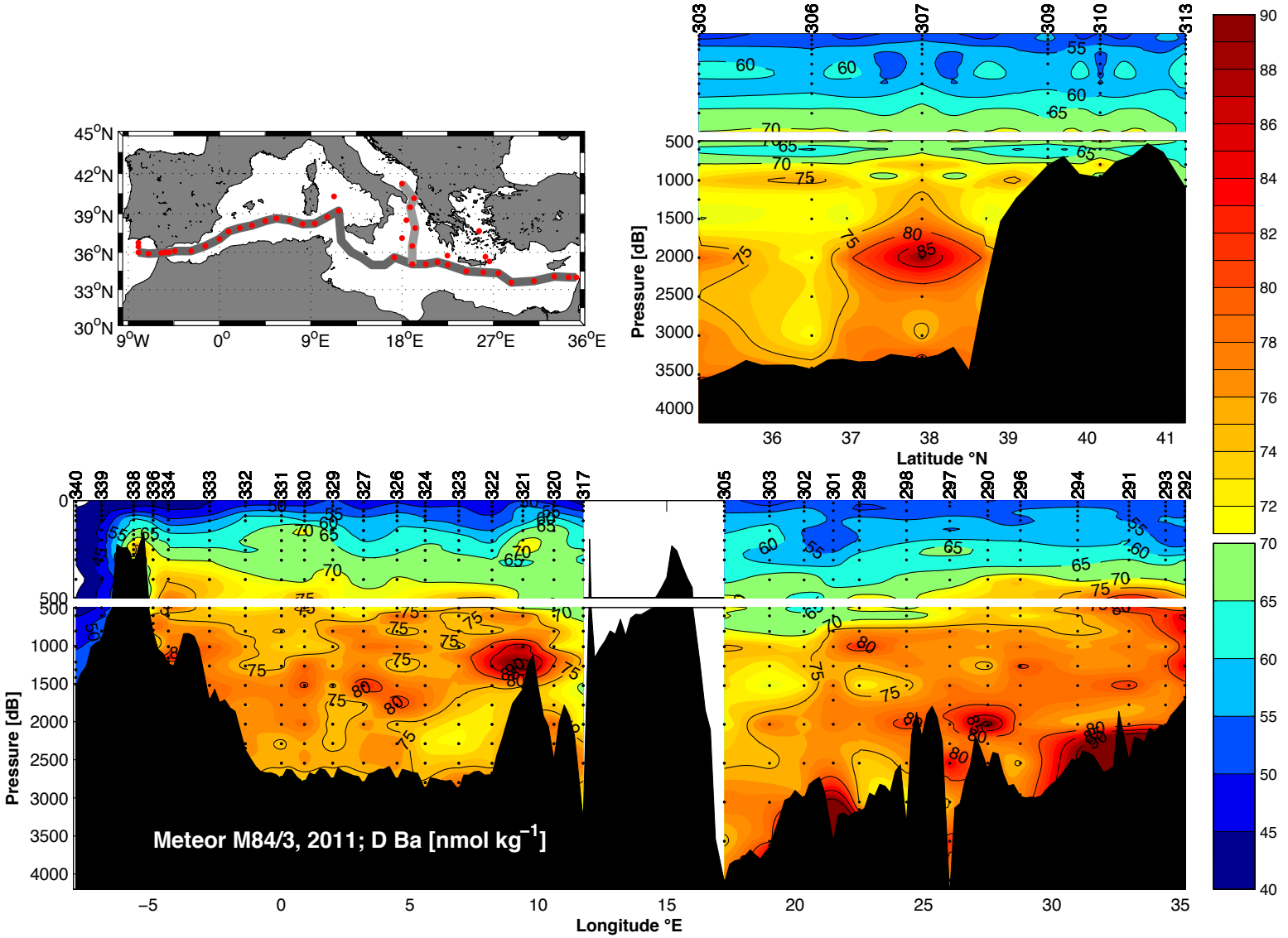
45°N
42°N
39°N
36°N
33°N
30°N
9°W
0°
9°E
18°E
27°E
36°E
Pressure [dB]
Latitude °N
Longitude °E
Meteor M84/3, 2011; D Ba [nmol kg$^{-1}$]

**Figure4**

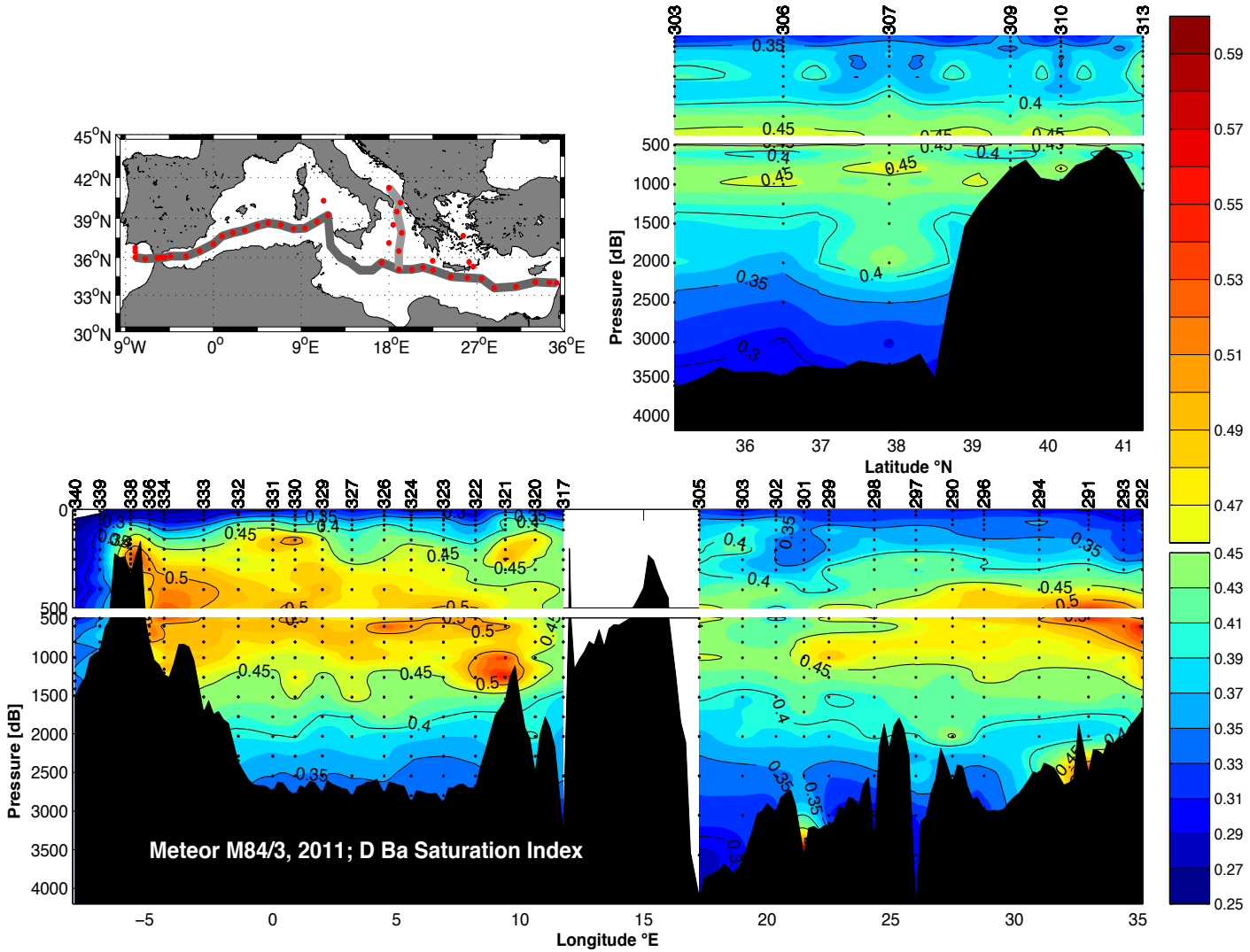
45°N
42°N
39°N
36°N
33°N
30°N
9°W
0°
9°E
18°E
27°E
36°E
Pressure [dB]
Latitude °N
Longitude °E
Meteor M84/3, 2011; D Ba Saturation Index

Figure5

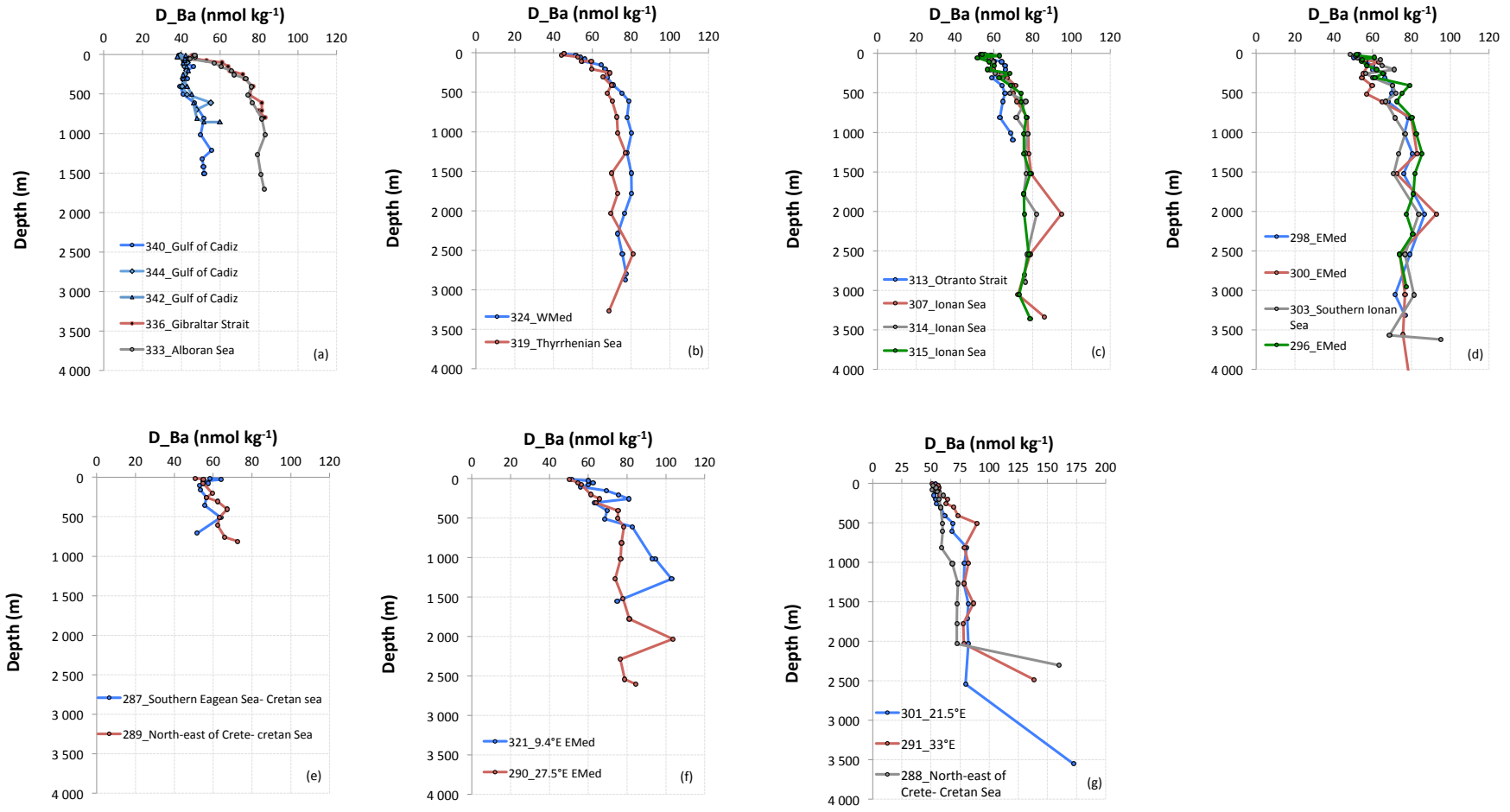
D_Ba (nmol kg-1)
Depth (m)
340_Gulf of Cadiz
344_Gulf of Cadiz
342_Gulf of Cadiz
336_Gibraltar Strait
333_Alboran Sea
(a)
324_WMed
319_Thyrrhenian Sea
(b)
313_Otranto Strait
307_Ionan Sea
314_Ionan Sea
315_Ionan Sea
(c)
298_EMed
300_EMed
303_Southern Ionan Sea
296_EMed
(d)
287_Southern Eagean Sea- Cretan sea
289_North-east of Crete- cretan Sea
(e)
321_9.4°E EMed
290_27.5°E EMed
(f)
301_21.5°E
291_33°E
288_North-east of Crete- Cretan Sea
(g)

***Research Highlights**

D_Ba is investigated along a high resolution and quasi-zonal transect in the MedSea.

The D_Ba content ranges from 38 to 85 nmol $kg^{-1}$ with local deep D_Ba maxima reaching up to 172 nmol $kg^{-1}$

The water column is largely undersaturated with respect to barite ($0.2<SI<0.6$).

The D_Ba distribution is impacted by the large-scale Mediterranean circulation and biogeochemical processes.

Local changes in the D_Ba patterns may be key to better constrain the C dynamics in the MedSea.